

Unraveling the Effect of Textured Contact Lenses on Iris Recognition

Daksha Yadav, *Student Member, IEEE*, Naman Kohli, *Student Member, IEEE*,
 James S. Doyle, Jr., *Student Member, IEEE*, Richa Singh, *Member, IEEE*,
 Mayank Vatsa, *Member, IEEE*, and Kevin W. Bowyer, *Fellow, IEEE*

Abstract—The presence of a contact lens, particularly a textured cosmetic lens, poses a challenge to iris recognition as it obfuscates the natural iris patterns. The main contribution of this paper is to present an in-depth analysis of the effect of contact lenses on iris recognition. Two databases, namely, the IIIT-D Iris Contact Lens database and the ND-Contact Lens database, are prepared to analyze the variations caused due to contact lenses. We also present a novel lens detection algorithm that can be used to reduce the effect of contact lenses. The proposed approach outperforms other lens detection algorithms on the two databases and shows improved iris recognition performance.

Index Terms—Iris recognition, contact lens, lens detection.

I. INTRODUCTION

IRIS is one of the most promising biometric modalities, and is in regular use in large-scale applications such as UAE port of entry and India's UIDAI (Aadhar) projects. While Flom and Safir [1] proposed the texture of the iris as a biometric modality in a 1987 patent, the first working iris biometric algorithm was developed in the early 1990s by John Daugman [2]. Daugman's approach was for a long time the basis for essentially all commercial iris recognition systems, and is still the most widely-used approach. Though iris features are unique, recent research results suggest that they are affected by several covariates such as pupil dilation [3] and sensor interoperability [4], [5]. Another factor that may affect iris recognition, which has received relatively less attention, is the presence of *transparent (soft)* and *color cosmetic (textured) contact lenses*. With recent developments in technology and low cost, the use of contact lenses is becoming more prevalent. According to Nichols [6], the number of contact lens wearers in the United States grew from around 34–36 million to

Manuscript received October 24, 2013; revised January 26, 2014; accepted March 11, 2014. Date of publication March 20, 2014; date of current version April 15, 2014. The associate editor coordinating the review of this manuscript and approving it for publication was Prof. Zhenan Sun.

D. Yadav and N. Kohli are with the Lane Department of Computer Science and Electrical Engineering, West Virginia University, Morgantown, WV 26501 USA (e-mail: dayadav@mix.wvu.edu; nakohli@mix.wvu.edu).

J. S. Doyle, Jr., and K. W. Bowyer are with the Department of Computer Science and Engineering, University of Notre Dame, Notre Dame, IN 46556 USA (e-mail: jdoyle6@nd.edu; kwb@nd.edu).

R. Singh and M. Vatsa are with the Indraprastha Institute of Information Technology Delhi, New Delhi 110078, India (e-mail: rsingh@iiitd.ac.in; mayank@iiitd.ac.in).

Color versions of one or more of the figures in this paper are available online at <http://ieeexplore.ieee.org>.

Digital Object Identifier 10.1109/TIFS.2014.2313025

37–38 million wearers and the worldwide number of contact lens wearers increased between 3%–5%.

It has long been believed that soft prescription contact lenses do not significantly affect the accuracy of iris recognition. For example, Negin et al. [8] have stated that “Successful identification can be made through eyeglasses and contact lenses.” However, since the purpose of a prescription contact lens is to change the optical properties of the eye, it must, by definition, have some effect on the iris texture observed through it [9]. In practice, contact lenses have been shown to reduce the overall accuracy of some iris biometrics systems [10]. A clear, soft, non-textured lens is also able to move relative to the iris, resulting in a marginally different observed effect on the iris texture at each presentation. Some soft lenses also have visible markings on them, which may be observed in different locations from image to image. Sometimes, lenses also have a noticeable boundary between the support region of the lens and the corrective region of the lens, which can also alter the appearance of the iris texture.

Contact lenses are generally used to correct eyesight as an alternative to spectacles/glasses. They are, however, also being used for cosmetic reasons, where the color and texture manufactured into a contact lens is superimposed on the natural texture and color of the iris. As shown in Fig. 1, it is apparent that the use of a textured lens changes the appearance/texture of an eye in both the visible and the near-infrared spectrums. The last panel in the figure also shows that in near-infrared, texture information is prominent in the textured contact lenses, and will obfuscate natural iris patterns. This example suggests that textured lenses can also be used as a spoofing mechanism. Detection of the presence of a contact lens is the first step to improving the usability and reliability of iris recognition for contact lens wearers. One simple solution might be to change the decision threshold when a clear non-textured contact lens is detected such that the false non-match rate (FNMR) is identical to users who do not wear lenses. Detection is also a first step to performing any sort of image correction on images with contact lens artifacts.

A. Literature Review

In 2003, Daugman [11] proposed using Fourier transform to detect periodic fake iris patterns that were prevalent in textured lenses manufactured at that time. Newer lenses however, have multiple layers of printing, making the Fourier response less

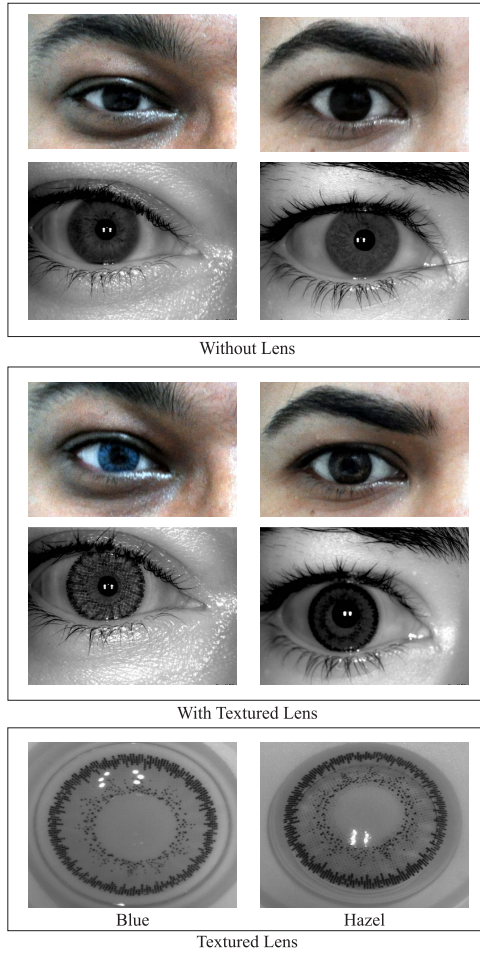


Fig. 1. Appearance of textured contact lenses. The top row in the “Without Lens” panel and in the “With Textured Lens” panel shows eye images in visible light. The bottom row in each panel shows the same eye images in near-infrared by a commercial iris sensor. The “Textured Lens” panel shows samples of color textured lenses imaged in near-infrared domain. Image adapted from [7].

pronounced and the textured lens detection by this method less reliable. Additionally, not all textured lenses use a dot-matrix style printing method.

Lee et al. [12] suggested that the Purkinje images would be different between a live iris and a fake iris. They proposed a novel iris sensor with structured illumination to detect this difference in Purkinje images. They reported results on a dataset of 300 genuine iris images and 15 counterfeit images. They reported a False Accept Rate (FAR) and False Reject Rate (FRR) of 0.33% on the data, but suggested that the dataset may be too small to draw generalized conclusions.

X. He et al. [13] proposed training a support-vector machine on texture features in a gray-level co-occurrence matrix (GLCM). They constructed a dataset of 2000 genuine iris images from the SJTU v3.0 database and 250 textured lens images, of which 1000 genuine lens images and 150 textured lens images were used for training. They reported a correct classification rate of 100% on the testing data. Using a similar approach, Wei et al. [14] analyzed three methods for textured contact lens detection: measure of iris edge sharpness, characterizing iris texture through Iris-Textons,

and co-occurrence matrix. Two class-balanced datasets were constructed using CASIA and BATH databases for genuine iris images and a special acquisition for textured contact lenses. Each dataset contained samples of a single manufacturer of textured contact lenses. Correct classification rates for the three methods and two datasets vary between 76.8% and 100%.

Z. He et al. [15] used multi-scale Local Binary Patterns (LBP) as a feature extraction method and AdaBoost as a learning algorithm to build a textured lens classifier. They acquired a dataset of 600 images with 20 different varieties of fake iris texture, a majority of which are textured contact lenses. A training set of 300 false iris images is combined with 6000 images from the CASIA Iris-V3 and ICE v1.0.

Similarly, Zhang et al. [16] investigated the use of Gaussian-smoothed and SIFT-weighted Local Binary Patterns to detect textured lenses in images acquired with multiple iris cameras. They constructed a dataset of 5000 fake iris images with 70 different textured lens varieties. They reported a correct classification rate of over 99% when training on heterogenous data, but this drops to 88% when different sensors are used for training and testing sets.

Preliminary versions of different parts of this paper have been individually published by Doyle et al. [17], [18] and Kohli et al. [7]. This work extends previous work by performing experiments on additional datasets, evaluating two contact lens detection algorithms on additional datasets, and evaluating the use of a contact lens detection algorithm to screen images from being sent for recognition processing.

B. Research Contributions

We believe that it is important to understand (1) the effect of contact lenses on the performance of iris recognition algorithms and (2) how this effect can be mitigated by appropriate detection schemes. The main contributions of this research are three fold:

- Preparing iris contact lens databases: IIIT-Delhi Contact Lens Iris database and ND Contact Lens Detection 2013 database,
- Documenting the effects of soft and textured contact lenses on iris recognition, and
- Evaluating the detection of textured contact lenses as a step in the processing flow for iris recognition.

II. DATABASES

The first major contribution of this research is the preparation of iris contact lens databases, namely IIIT-D Contact Lens Iris¹ and ND Contact Lens Detection 2013², for analysis and algorithm development purposes. These two databases are complementary in terms of ethnicity of volunteers, lens makers and models, and iris sensors. IIIT-D Contact Lens Iris Database provides an in-depth analysis of the effect of contact lenses since each user has non-lens, soft lens, and textured

¹The IIIT-Delhi Contact Lens Iris Database is available upon request. Access information can be found at <https://research.iitd.edu.in/groups/fab/irisdatabases.html>.

²The ND Contact Lens Database 2013 is available upon request. Access information can be found at http://www3.nd.edu/cvrl/CVRL/Data_Sets.html

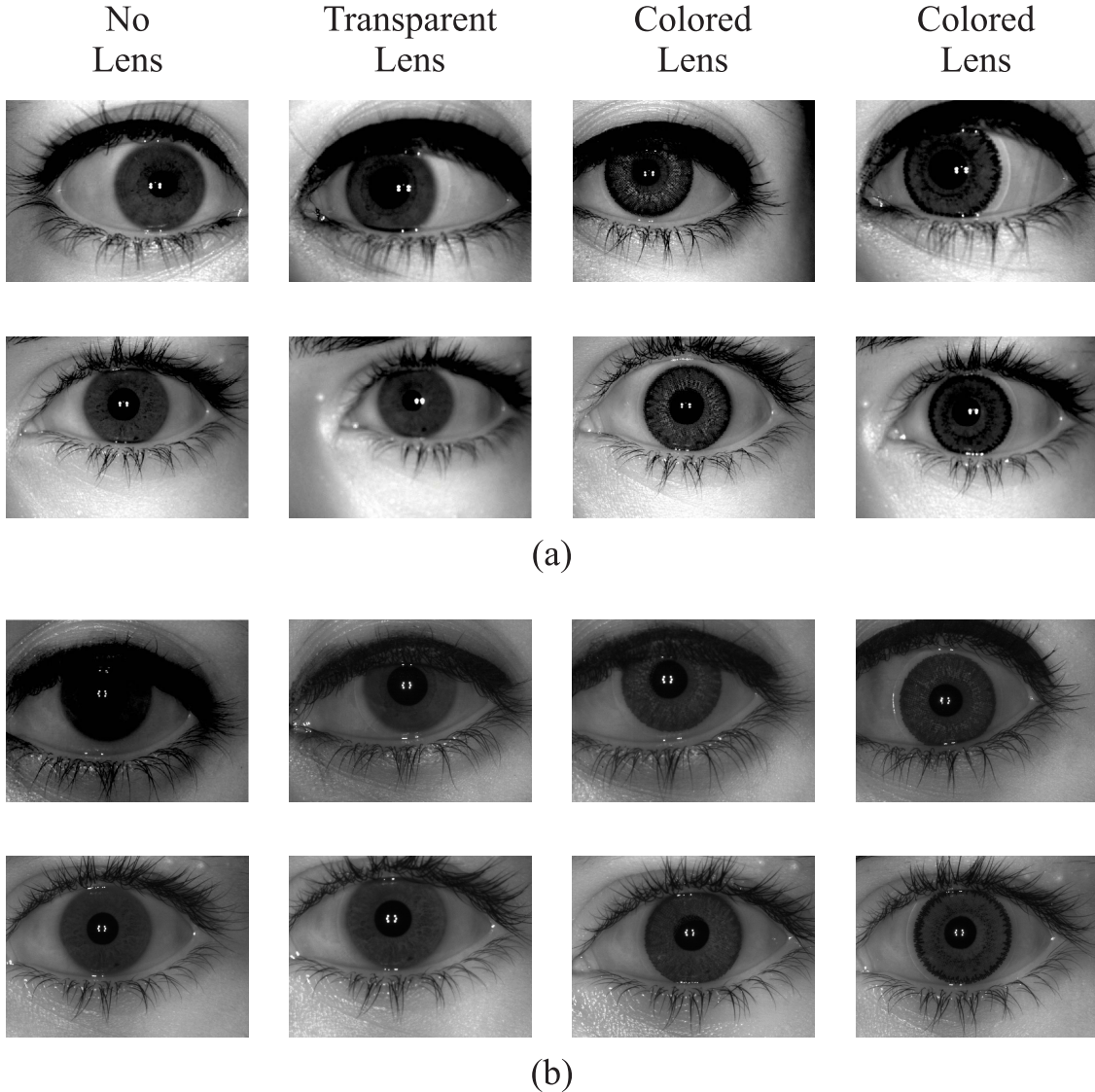


Fig. 2. Iris images in IIIT-D Contact Lens Iris Database (IIIT-D CLI): (a) images captured using Cogent iris sensor and (b) images captured using Vista iris sensor. The two textured lenses used here are from CIBA Vision in third column and Bausch & Lomb in fourth column.

lens images in the database. This data arrangement makes it ideal for plotting ROC curves for the cases when textured lens detection is not in use and when it is in use to see the performance difference. At the same time, ND Contact Lens Detection 2013 database provides a holistic view of the contact lenses because it has varying makes and models of contact lens which makes it ideal for analyzing lens detection algorithms. No subject who is wearing a cosmetic lens appears without a cosmetic lens. This arrangement allows for classifiers to be trained on the lens features rather than potentially training on subject features. The details for both the databases are presented below. Both datasets are available to the research community. To our knowledge (and as reported in [11]–[16]) these are the first cosmetic contact lens datasets to be made available to the research community.

A. IIIT-D Contact Lens Iris Database

The IIIT-D Contact Lens Iris (IIIT-D CLI) database is prepared with three objectives: (1) capture images pertaining

TABLE I
DETAILS OF THE IIIT-D CONTACT LENS IRIS DATABASE

Number of subject eyes	202
Types of contact lens	None, soft, and textured
Lens manufactures	CIBA Vision and Bausch & Lomb
Lens colors	Blue, Gray, Hazel and Green
Number of subjects per textured lens type	Blue (20), Gray (29), Green (30) and Hazel (22)
Iris sensors used for acquisition	Cogent dual iris sensor and VistaFA2E iris sensor
Number of images per subject per lens type	Minimum 3 images per eye class, per lens type
Total number of images in the database	6570
Download Link	http://research.iiitd.edu.in/groups/iab/irisdatabases.html

to at least 100 subjects, (2) for each individual, capture images without lens, with soft (prescription) lens, and with textured lens, and (3) capture images with variations in iris sensors and lenses (colors and manufacturers). Table I

TABLE II
DETAILS OF THE NDCLD'13 CONTACT LENS DETECTION DATABASE

Number of subject eyes	I: 287 II: 89
Types of contact lens	None, soft, and textured
Lens manufactures	CIBA Vision, Johnson&Johnson, Cooper Vision
Lens colors	Blue, Gray, Honey and Green
Iris sensors used for acquisition	LG4000, IrisGuard AD100
Total number of image in the database	5100
Download Link	http://www3.nd.edu/~cvrl/CVRL/Data_Sets.html

summarizes the characteristics of the IIIT-D CLI database which is comprised of 6570 iris images pertaining to 101 subjects. Both left and right iris images of each subject are captured and therefore, there are 202 iris classes. The lenses used in the database are soft lenses manufactured by CIBA Vision [19] and Bausch&Lomb [20]. For textured lenses, four colors are used. To study the effect of the acquisition device on contact lenses, iris images are captured using two iris sensors: (1) Cogent dual iris sensor (CIS 202) and (2) VistaFA2E single iris sensor. The database contains a minimum of three images for each iris class in each of the above mentioned lens categories for both the iris sensors. Fig. 2 shows the sample images from IIIT-D CLI database.

B. ND Contact Lens Detection 2013 Database

The ND Contact Lens Detection 2013 (NDCLD'13) database consists of 5100 images and is conceptually divided into three datasets for further evaluation. Dataset I consists of a training set of 3000 images and a verification set of 1200 images, all acquired with an LG 4000 [21] iris camera. Both the training set and the verification set are divided equally into three classes: (1) no contact lenses, (2) soft, non-textured contact lenses, and (3) textured contact lenses. Classes (1) and (2) are balanced between male and female, and represent a variety of ethnicities. Category (3) images are predominantly from Caucasian males. Dataset II consists of a training set of 600 images and a verification set of 300 images, all images acquired with an IrisGuard AD100 [22] iris camera. Again, the dataset is balanced across the three categories in the same manner. Dataset III is simply the union of Dataset I and Dataset II resulting in a multi-camera training set of 3600 images and a verification set of 1500 images. Fig. 3 shows sample images from Dataset I and Fig. 4 shows samples from Dataset II. A summary of NDCLD'13 can be found in Table II.

All textured contact lenses in this dataset came from three major suppliers: Johnson&Johnson [23], CIBA Vision [19], and Cooper Vision [24]. Subjects in the database belong to four different ethnic categories (Caucasian, Asian, Black, and Other). Multiple colors of contact lenses were selected for each manufacturer. Some were also “toric” lenses, meaning that they are designed to correct for astigmatism. Toric lenses are designed to maintain a preferred orientation around the optical axis. As such, they may present different artifacts than

non-toric lenses but also may have less variation in the position on the eye.

III. EFFECTS OF CONTACT LENSES ON IRIS RECOGNITION

Many types and colors of lenses are available from a number of different manufacturers. To analyze the effect of these parameters on iris recognition, we have conducted a performance evaluation using the VeriEye [25], commercial iris recognition system. Two sets of experiments are performed on the IIIT-D CLI database to evaluate the iris verification performance:

- 1) *Effect of soft and textured lenses:* By varying the gallery probe combinations, the effect of different types of lenses on iris verification is analyzed.
- 2) *Effect of acquisition device:* This experiment is performed to analyze whether iris acquisition using different sensors has any effect on the performance with contact lens variations. Three experiments are performed:
 - a) both the gallery and probe images are captured using the Cogent sensor
 - b) both the gallery and probe images are captured using the Vista sensor
 - c) cross sensor gallery - probe verification experiment.

The verification accuracies of VeriEye are computed for the above mentioned protocols and the results are shown in Fig. 5 and Tables III–V. The key results are summarized as follows:

- In the case of no contact lens in either the gallery or the probe image, the verification rate with images from either sensor, and from cross-sensor, is similar and quite high.
- In the case of gallery and probe images both having soft contact lenses, the verification rate of matching images from both sensors is again high. However, the cross-sensor performance is greatly degraded, showing only 47% verification accuracy. This suggests that the sensors somehow react differently to the presence of contact lenses in the scene. Both the sensors can handle the presence of soft contacts for matching same-sensor images, but they handle soft lenses differently enough that cross-sensor matching gives a much worse verification rate.
- In the case of no contact lens being compared with soft contact lens, the none-soft and soft-none entries in Table III, the verification rate obtained with the Cogent images is high, but the rate obtained with images from the Vista sensor, and also the cross-sensor verification rate, is low.
- In the case of matching images with no contact lens and images with textured contact lens, the verification rate is below 40% in all cases. The same situation holds for matching images with a soft lens against images with a textured lens. These are cases where iris recognition is stymied in general by the fact that the textured contact lens superimposes its texture over the natural iris texture. (See examples in Figure 6.)
- In the case of matching a textured lens in the gallery against a textured lens probe, verification rates for both



Fig. 3. Sample LG400 images for the three classes showing the original images and the unrolled sections from which the features were extracted. The no lens images were taken from sample 05629d33. The soft lens images were taken from sample 05675d5684. The textured lens images were taken from sample 04261d2211. Reproduced with permission from [18]. (a) No Lens - Full. (b) Soft Lens - Full. (c) Textured Lens - Full. (d) No Lens - Pupil. (e) Soft Lens - Pupil. (f) Textured Lens - Pupil. (g) No Lens - Iris. (h) Soft Lens - Iris. (i) Textured Lens - Iris. (j) No Lens - Sclera. (k) Soft Lens - Sclera. (l) Textured Lens - Sclera

sensors are much lower than matching images with no lenses, but are also significantly higher than matching images with no lens against images with a textured lens. At the same time, the cross-sensor verification rate is the lowest of all the cases considered, only 5%. The verification rate in this case is strong evidence against the idea that the texture pattern in a particular type of textured contact can be enrolled in order to recognize the presence of that contact lens in an image.

A similar experiment was conducted for the NDCLD'13 Dataset. ROC curves were computed for three conditions: (1) no contact lens in gallery image or probe image, (2) soft contact lens in both gallery image and probe image, and (3) textured contact lens in both gallery image and probe image. The ROC curves computed using VeriEye are plotted together in Figs. 7 and 8. Conclusions from this experiment can be summarized as follows:

- The best recognition accuracy is obtained in the case of no contact lens in both the gallery and probe images or a soft contact lens in both the gallery or the probe images.
- Recognition accuracy in the case of textured contact lenses in the gallery and probe image is greatly reduced

TABLE III
VERIFICATION RESULTS WITH VARIATIONS IN ACQUISITION DEVICE
AND LENS TYPE. VERIFICATION % IS REPORTED AT 0.01% FAR

Lens type/ Sensor (Gallery/Probe)	Cogent	Vista	Cross Sensor
None - None	98.9	99.8	97.9
None - Soft	96.1	59.9	95.0
None - Textured	22.1	36.4	23.4
Soft - Soft	96.4	99.8	47.3
Soft - None	96.1	57.4	48.8
Soft - Textured	22.9	33.8	22.5
Textured - Textured	50.4	63.3	5.0
Textured - None	23.0	38.2	20.4
Textured - Soft	22.8	32.8	17.3

relative to the case of no contact lenses in either image and to the case of soft contacts in both images.

These conclusions based on experiments with the ND database agree with the conclusions of the experiments on the IIIT-D database. Given that the two datasets involve different sensors, different subjects, and also different brands of contact lenses, and that the experiments were run at different institutions, the shared conclusions should have very high confidence.



Fig. 4. Sample AD100 images for the three classes showing the original images and the unrolled sections from which the features were extracted. The no lens images were taken from sample 05629d932. The soft lens images were taken from sample 05675d1366. The textured lens images were taken from sample 04261d3849. Reproduced with permission from [18]. (a) No Lens - Full. (b) Soft Lens - Full. (c) Textured Lens - Full. (d) No Lens - Pupil. (e) Soft Lens - Pupil. (f) Textured Lens - Pupil. (g) No Lens - Iris. (h) Soft Lens - Iris. (i) Textured Lens - Iris. (j) No Lens - Sclera. (k) Soft Lens - Sclera. (l) Textured Lens - Sclera.

TABLE IV
MINIMUM, MAXIMUM, MEAN GENUINE AND IMPOSTOR SCORES
OBTAINED FROM VERIEYE [25] FOR DIFFERENT LENS
TYPES FOR COGENT SCANNER

Lens	Genuine		Impostor	
	[Min, Max]	Mean	[Min, Max]	Mean
None	[0, 1550]	653.19	[0, 87]	0.02
Soft	[0, 1345]	472.99	[0, 447]	0.03
Blue Color	[0, 180]	31.76	[0, 77]	0.03
Hazel Color	[0, 129]	20.66	[0, 67]	0.01
Green Color	[0, 166]	22.86	[0, 79]	0.01
Gray Color	[0, 160]	17.82	[0, 96]	0.03

TABLE V
MINIMUM, MAXIMUM, MEAN GENUINE AND IMPOSTOR SCORES
OBTAINED FROM VERIEYE [25] FOR DIFFERENT LENS
TYPES FOR VISTA SCANNER

Lens	Genuine		Impostor	
	[Min, Max]	Mean	[Min, Max]	Mean
None	[0, 3253]	657.22	[0, 58]	3.04
Soft	[0, 1284]	468.49	[0, 858]	3.11
Blue Color	[0, 140]	43.13	[0, 57]	3.11
Hazel Color	[0, 160]	34.51	[0, 57]	3.06
Green Color	[0, 191]	41.48	[0, 77]	3.07
Gray Color	[0, 203]	47.02	[0, 55]	3.05

IV. ALGORITHMS AND RESULTS FOR LENS DETECTION

Textured contact lenses are designed to alter the appearance of the wearer's eye, giving it a different color and/or texture.

Unfortunately, they also greatly reduce the amount of genuine iris texture visible to iris recognition systems. This increases the chance of a false non-match and a false match. Accordingly, these images should be rejected before a template is generated for them. The effect of soft lenses is much less. The genuine iris texture is not concealed to the same extent it is with textured contact lenses. However, the negative impact on verification by soft lens wearers has been documented [7], [10].

It is our hypothesis that applying a lens detection algorithm to first reject the cases with *obfuscated* patterns and allowing only without lens and soft lens iris images can improve the performance of iris recognition algorithms and reduce the false matches at higher verification rates. To test this hypothesis, the experiment was conducted and the performance of the iris recognition was then evaluated.

A. Modified LBP Based Classification

The algorithm can be divided into two parts: feature extraction and model training.

1) *Feature Extraction:* Each iris image is divided into three regions: (1) pupil, (2) iris, and (3) sclera. For the NDCLD'13 dataset, the segmentation information is provided. For the IIIT-D dataset, the segmentation is obtained using a commercially available iris recognition SDK³. Segmentation

³Licensing agreements with the vendor of this SDK do not permit it to be named in this work.

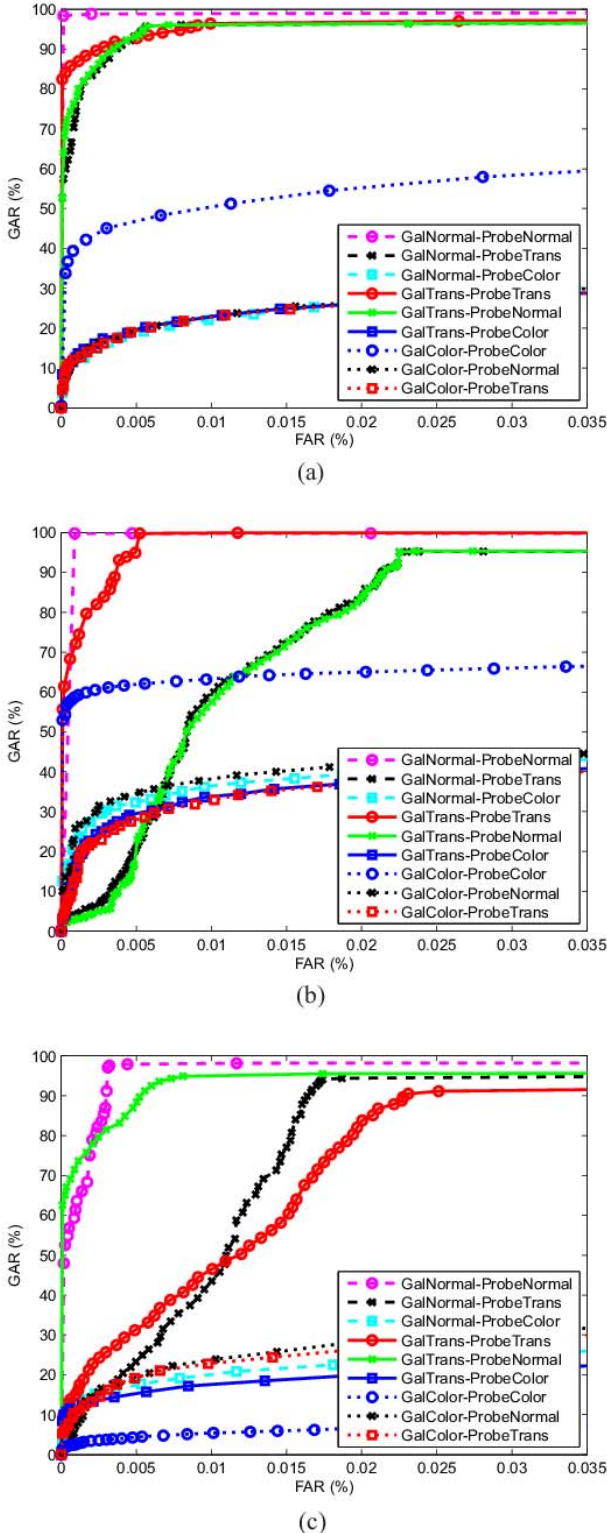


Fig. 5. ROC curves for various experiments using VeriEye: (a) both the gallery and probe images are captured using the Cogent sensor, (b) both the gallery and probe images are captured using the Vista sensor, and (c) cross sensor matching. Reproduced with permission from [7].

for each image was verified by hand and adjusted manually in the case of large segmentation errors. Examples of the regions after extraction can be found for LG4000 sensor in Fig. 3 and AD100 sensor in Fig. 4. The boundaries of the sclera region

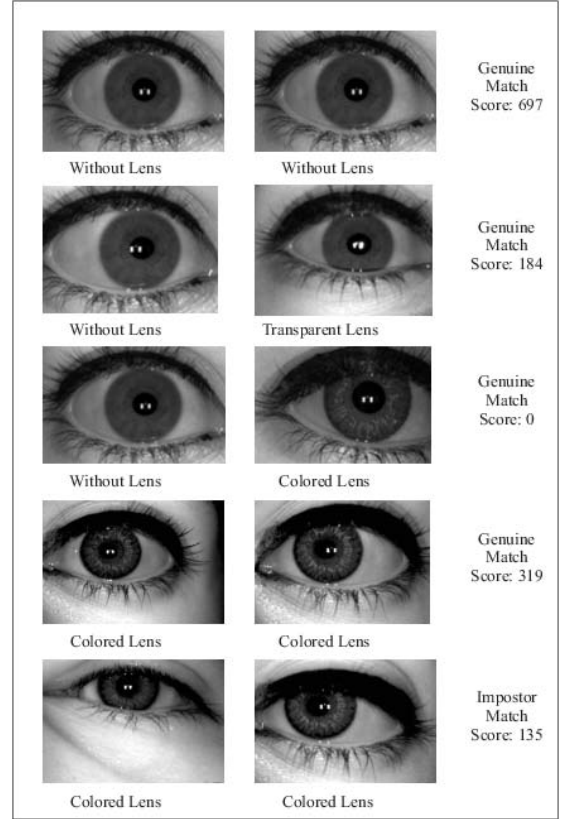


Fig. 6. Illustrating the effect of contact lenses on iris matching performance. Reproduced with permission from [7].

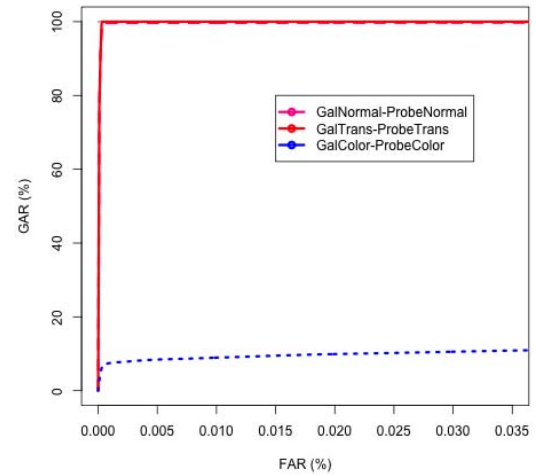


Fig. 7. ROC curves for the three classes in the NDCLD'13 Dataset I as determined by VeriEye [25]. The GalNormal-ProbeNormal and GalTrans-ProbeTrans overlap significantly for FAR range shown.

are determined by two circles with the same center point as the limbic circle but with different radii. The inner radius is 20px smaller than the limbic boundary and the outer radius is 60px larger than the limbic boundary in original image coordinates in an attempt to capture contact lens boundaries that may have shifted into the iris region while also limiting the amount of eyelid and eyelash occlusion.

Modified Local Binary Pattern analysis (similar to [26]) is applied to each of the three regions of each image at

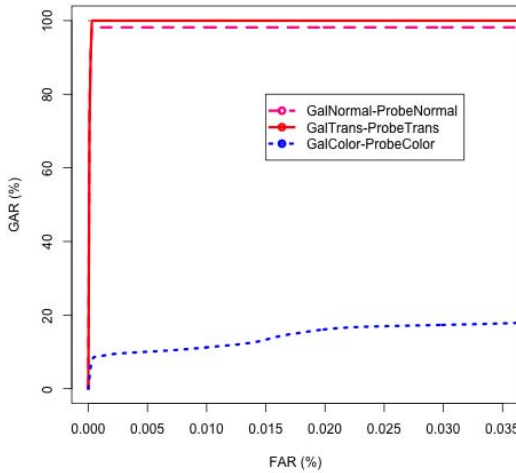


Fig. 8. ROC curves for the three classes in the NDCLD'13 Dataset II as determined by VeriEye [25].

multiple scales to produce feature values. Unlike traditional LBP, this method does not decompose the image into blocks and independently analyze each block to construct a large feature vector. Instead, the extracted region is treated as one large block. The kernel size for the binary pattern analysis is scaled from 1 to 20 in increments of 1 for a total of 20 different feature sets for each of the three regions and 60 feature sets overall.

2) *Model Training:* 17 different classifiers, (see Table VI), intentionally sampling a variety of different classifier technologies [27], were explored as possible approaches to train models on the feature sets. Each of the feature sets described in feature extraction is treated as an independent dataset for the purposes of model training.

For machine learning algorithms that had tunable parameters, a grid search was performed with reasonable values. The predefined folds for each dataset are used to evaluate the performance of each trained model by cross-fold evaluation. If a classifier yielded a correct classification rate (CCR) of 100% on all 10 folds, a model was built using all training data. This process resulted in an ensemble of trained models to be evaluated on the verification set.

We also compared the proposed algorithm with other pre-existing techniques in the literature such as textural features based on Co-occurrence Matrix [14], GLCM based analysis [13], weighted LBP approach [16], as well as texture classification techniques such as LBP [26] with SVM classification, and fusion of LBP and PHOG [28] (when LBP and PHOG are concatenated to obtain fused descriptor). (See examples in Figures 9 and 10.) Each algorithm was implemented by the authors of this paper, except weighted LBP for which the source code was supplied by the authors of [16].

B. Results

The problem of lens detection in an iris image is approached as a three class classification problem: no lens, soft lens, and textured lens. Three types of experiments were performed to evaluate the correct classification rate of the constructed model

TABLE VI
LIST OF WEKA CLASSIFIERS USED IN MODEL TRAINING. CCR FOR INDIVIDUAL CLASSIFIERS ON THE VERIFICATION PORTION OF DATASET I OF NDCLD'13

Weka Classifier Name	2-class CCR
Naive Bayes	35.33%
Logistic	87.66%
Multilayer Perceptron	33.33%
Simple Logistic	86.66%
SMO	33.33%
IBk	33.33%
Bagging	75.67%
Logit Boost	93.67%
Decision Table	74.00%
JRip	33.33%
OneR	33.33%
PART	33.33%
Ridor	33.33%
FT	96.00%
J48	33.33%
Random Forest	54.33%
Random Tree	33.66%

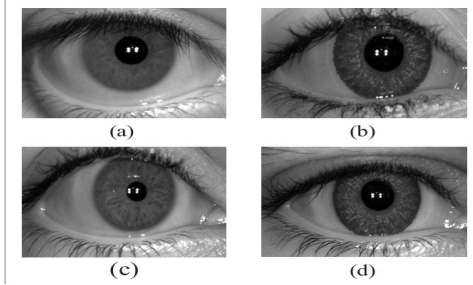


Fig. 9. Examples of correct (a: without lens and b: textured lens) and incorrect classifications (c: without lens as textured lens and d: textured lens as without lens) using co-occurrence matrix [14]. Reproduced with permission from [7].

ensembles on all four datasets: IIIT-D Cogent, IIIT-D Vista, ND Dataset-I and II. They include the intra-sensor case, inter-sensor cases and multi-sensor cases. The results for the same are mentioned below.

1) *Intra-Sensor Validation:* The performance of the ensembles built for all training datasets is evaluated on the corresponding verification sets. For each image of each verification set, a prediction and a confidence is output by each of the model ensembles. A final prediction for each image is decided by taking the maximum of the sum of confidences for each ensemble for each class. All datasets perform about equally in the intra-sensor experiment.

- For IIIT-D Dataset Cogent, the final ensemble resulted in a CCR of over 73% on the three-class problem. The accuracy of detecting instances of textured contact lenses was again quite high, nearly 95%.
- For IIIT-D Dataset Vista, the final ensemble resulted in a CCR of 80% on the three-class problem. The accuracy of detecting instances of textured contact lenses was again high, nearly 92%.
- For ND Dataset I, the final ensemble resulted in a CCR of over 75% on the three-class problem. The accuracy of detecting instances of textured contact lenses was quite high, nearly 97%.

TABLE VII
LENS CLASSIFICATION RESULTS OF PROPOSED ALGORITHM AND COMPARISON WITH OTHER APPROACHES (IN %)
WHERE N-N IS NONE-NONE, T-T IS TEXTURED-TEXTURED AND S-S IS SOFT-SOFT

Database	Classification Type	Textural Features [14]	GLCM Features [13]	Weighted LBP [16]	LBP + SVM	LBP + PHOG + SVM	mLBP
IIITD Cogent	N-N	33.28	32.76	45.39	65.53	59.73	66.83
	T-T	77.78	45.44	85.41	89.39	91.87	94.91
	S-S	42.73	33.34	54.43	42.73	52.84	56.66
	Total	51.63	37.31	62.06	66.40	68.57	73.01
IIITD Vista	N-N	79.75	53.99	43.15	53.37	49.49	76.21
	T-T	94.36	60.12	90.67	98.64	99.42	91.62
	S-S	16.43	0.0	56.11	50.90	59.32	67.52
	Total	63.73	32.69	63.72	68.04	69.84	80.04
ND I	N-N	78.00	73.75	57.00	70.00	81.25	85.00
	T-T	86.00	62.25	89.50	97.00	96.25	96.50
	S-S	35.84	3.75	51.27	60.15	65.41	45.25
	Total	66.72	46.62	65.88	75.73	80.98	75.58
ND II	N-N	47.00	33.00	47.00	42.00	42.00	81.00
	T-T	86.00	93.00	82.00	100.00	96.00	100.00
	S-S	0.00	67.00	44.0	54.00	60.00	52.00
	Total	44.33	64.33	57.67	65.33	66.00	77.67

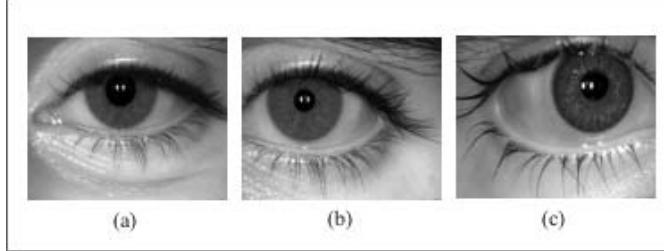


Fig. 10. Misclassification by LBP + PHOG and SVM classification: (a) without lens image classified as image with soft lens, (b) image with soft lens classified as without lens, and (c) image with textured lens classified as image with soft lens.

- For ND Dataset II, the final ensemble resulted in a CCR of over 77% on the three-class problem. The accuracy of detecting instances of textured contact lenses was 100%.

The results of the intra-sensor experiments are summarized in Table VII. As can be seen from the Table, the proposed algorithm out-performs all the algorithms tested on all the databases except the ND-Database I. The fusion algorithm of LBP and PHOG performs better on the Database I due to its higher detection rate for soft lenses in this scenario.

2) *Inter-Sensor Validation*: In this scenario, models trained on one dataset were tested on the other to see the interoperability performance of the algorithm. We compared the pairwise comparisons of Dataset I and II, and Database Cogent and Vista. Three of the four datasets perform worse than in the intra-sensor experiment. The models trained on Dataset Cogent and evaluated on Dataset Vista did not experience a large drop in performance. The accuracy for all of the experiments can be found in Table VIII.

- With inter-sensor validation results when trained on IIIT-D Dataset Vista and tested on IIIT-D Dataset Cogent, the final ensemble resulted in a CCR of 65% on the three-class problem, a significant drop in performance over the intra-sensor validation. The accuracy of detecting instances of textured contact lenses also dropped to nearly 81%.
- With inter-sensor validation results when trained on IIIT-D Dataset Cogent and tested on IIIT-D Dataset Vista, the final ensemble resulted in a CCR of 77% on the three-class problem, a slight drop in performance over the intra-sensor validation. The accuracy of detecting instances of textured contact lenses stayed constant at nearly 93%.
- With inter-sensor validation results when trained on ND Dataset I and tested on ND Dataset II, the final ensemble resulted in a CCR of 61% on the three-class problem, a significant drop in performance over the intra-sensor validation. The accuracy of detecting instances of textured contact lenses also dropped to 93%.
- With inter-sensor validation results when trained on ND Dataset II and tested on ND Dataset I, the final ensemble resulted in a CCR of 60% on the three-class problem, a significant drop in performance over the intra-sensor validation. The accuracy of detecting instances of textured contact lenses also dropped to just over 88%.

3) *Multi-Sensor Validation*: The intra-sensor and inter-sensor experiments show that trained mLBP models are sensor-specific and do not generalize to novel sensors. The following results report correct classification rates for models that are trained with a training set containing images from multiple sensors and then evaluated on a verification set of

TABLE VIII

LENS CLASSIFICATION RESULTS OF PROPOSED mLBP ALGORITHM (IN %) WHERE N-N IS NONE-NONE, T-T IS TEXTURED-TEXTURED AND S-S IS SOFT-SOFT

Database	Models	Classification type	mLBP
IIITD Cogent	IIITD Vista	N-N	65.99
		T-T	80.81
		S-S	48.31
Total		65.29	
IIITD Vista	IIITD Cogent	N-N	62.10
		T-T	92.95
		S-S	75.44
Total		77.79	
ND I	ND II	N-N	62.25
		T-T	88.50
		S-S	29.50
Total		60.08	
ND II	ND I	N-N	74.00
		T-T	93.00
		S-S	17.00
Total		61.33	

images from the same set of multiple sensors. These results show that it is possible to retain the higher CCR of the intra-sensor experiment even when images from multiple sensors are present. (See results in Table IX.)

The performance of the ensembles built for the combined training datasets is evaluated on combined verification sets. For each image of the verification sets, a prediction and a confidence is output by each of the model ensembles. A final prediction for each image is decided by taking the maximum of the sum of confidences for each ensemble for each class. The performance on the combined datasets is in line with the performance of each individual dataset in the intra-sensor evaluation.

- With multi-sensor validation results when trained on IIIT-D Dataset Combined and tested on IIIT-D Dataset Combined data, the final ensemble resulted in a CCR of 73% on the three-class problem, only slightly less than in the intra-sensor experiments. The accuracy of detecting instances of textured contact lenses was constant at 95%.
- With multi-sensor validation results when trained on ND Dataset III and tested on ND Dataset III data, the final ensemble resulted in a CCR of 73% on the three-class problem, only slightly less than in the intra-sensor experiments. The accuracy of detecting instances of textured contact lenses also dropped slightly to 95%.

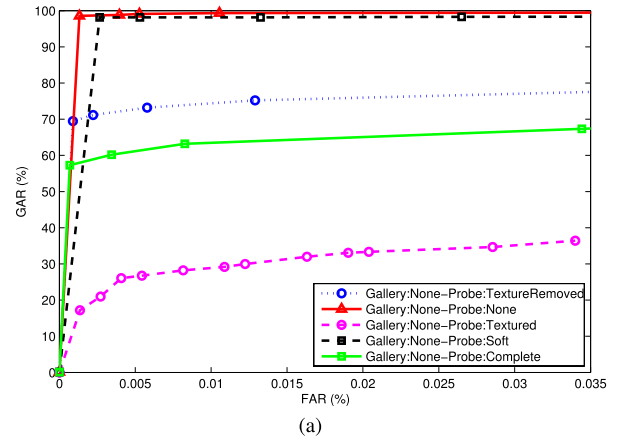
V. EFFECT OF LENS DETECTION ON IRIS RECOGNITION PERFORMANCE

To evaluate the proposition that “detecting and rejecting the iris samples with textured contact lens can improve the performance of iris recognition algorithms”, another experiment is performed in which the output of lens classification algorithm is provided as input to the iris recognition system. In this experiment, the gallery contains iris images without lens

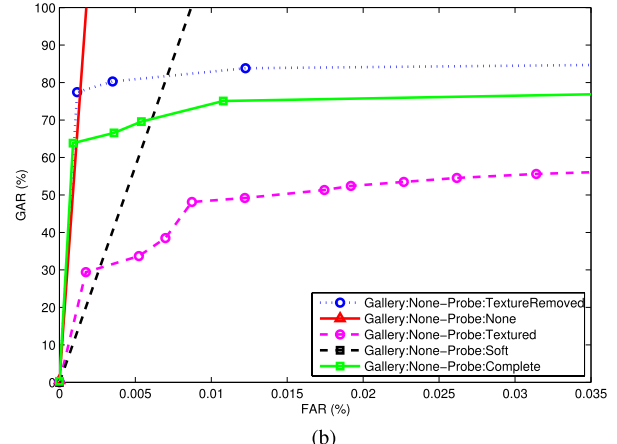
TABLE IX

LENS CLASSIFICATION RESULTS OF PROPOSED mLBP ALGORITHM ON THE COMBINED DATASETS (IN %) WHERE N-N IS NONE-NONE, T-T IS TEXTURED-TEXTURED AND S-S IS SOFT-SOFT

Database	Classification type	mLBP
IIITD Combined	N-N	62.14
	T-T	94.74
	S-S	61.63
Total		72.96
ND III	N-N	72.60
	T-T	97.00
	S-S	50.00
Total		73.20



(a)



(b)

Fig. 11. ROC curves demonstrating the effectiveness of incorporating proposed lens detection algorithm (Modified LBP based classification) with VeriEye. ‘Probe: TexturedRemoved’ refers to the scenario where textured lens detected iris images are removed from the probe. ‘Probe: Complete’ refers to the case when all three types of iris images are included in the probe in equal proportion. Rest of the cases demonstrate where each of the three types of iris images are included individually in the probe.

and the probe contains images without lens, with soft lens, and with textured lens separately. During probe verification (lens detection phase), the images classified as textured lens are declared as “failure to process” and we disregard them from our evaluations. We have used the proposed algorithm as the lens detection algorithm. Fig. 11 shows the ROC curves

obtained with this protocol and compares with the results obtained when the gallery image is without lens and all the probe images are classified as without lens classification and helps in mitigating the effect of textured lenses. Also, the performance when probe is only without any lens (none), only soft lens (without classification), and only textured lens (without classification) is shown. The results suggest that detection and removal of images with textured contact lens leads to an increase in the recognition accuracy as compared to without lens classification. However, it is still lower than the accuracy of none-none and soft-none gallery probe pairs due to less accurate lens detection algorithm.

VI. CONCLUSION

Wearing of contact lenses, both soft contacts and textured "cosmetic" soft contacts, degrades the accuracy of iris recognition. With clear soft contacts, the effect is a relatively small increase in the false non-match rate. With textured contact lenses, the effect is a major increase in the false non-match rate. At a false match rate of 1 in 1 million, which is an often-quoted operating point for iris recognition, textured contacts can cause the false-non-match to exceed 90%. Therefore, textured contact lenses could provide an effective way for someone on an iris recognition watch list to evade detection.

This paper combines the efforts of two research groups to analyze the effect of contact lenses on the performance of iris recognition. Two different contact lens iris image datasets have been collected, independently in different countries, using different iris sensors and sampling different brands of contact lenses. One contribution of this work is that the two datasets are being made available to the research community.

The datasets are used in a parallel set of experiments to explore the effects of contact lenses on iris recognition. Common conclusions include the following:

- Wearing clear soft contact lenses degrades iris recognition slightly relative to wearing no lenses.
- Wearing textured contact lenses degrades iris recognition significantly.
- Textured contact lenses can be automatically detected at a level of 95% accuracy or greater, for a wide range of sensors and a wide range of contact lens manufacturers, provided that the various brands of lenses are all represented in the training data.
- Detecting textured contact lenses and filtering them out of the stream for automated iris recognition can help in alleviating spoofing attempts. However, greater accuracy in detection of textured lenses is still needed.

The work reported in this paper is unique in combining the efforts of two research groups pursuing a common topic; in making large contact lens iris image datasets available to the research community; and in the range of iris sensors and contact lens manufacturers sampled.

ACKNOWLEDGMENT

The authors would like to thank Dr. Zhenan Sun for sharing the code for [16] used for comparison. The authors would also

like to thank the anonymous reviewers for offering feedback and suggestions that improved the paper.

REFERENCES

- [1] L. Flom and A. Safir, "Iris recognition system," U.S. Patent 4 641 349, Feb. 3, 1987.
- [2] J. Daugman, "How Iris recognition works," *IEEE Trans. Circuits Syst. Video Technol.*, vol. 14, no. 1, pp. 21–30, Jan. 2002.
- [3] K. Hollingsworth, K. W. Bowyer, and P. J. Flynn, "Pupil dilation degrades Iris biometric performance," *Comput. Vis. Image Understand.*, vol. 113, no. 1, pp. 150–157, 2009.
- [4] S. S. Arora, M. Vatsa, R. Singh, and A. K. Jain, "On Iris camera interoperability," in *Proc. BTAS*, 2012, pp. 346–352.
- [5] R. Connaughton, A. Sgroi, K. Bowyer, and P. Flynn, "A multialgorithm analysis of three Iris biometric sensors," *IEEE Trans. Inf. Forensics Security*, vol. 7, no. 3, pp. 919–931, Jan. 2012.
- [6] J. J. Nichols. (2012). *Annual Report: Contact Lenses* [Online]. Available: <http://www.clspectrum.com/articleviewer.aspx?articleID=107853>
- [7] N. Kohli, D. Yadav, M. Vatsa, and R. Singh, "Revisiting Iris recognition with color cosmetic contact lenses," in *Proc. 6th IAPR*, 2013, pp. 1–5.
- [8] M. Negin, T. Chmielewski, M. Salganicoff, U. von Seelen, P. Venetainer, and G. Zhang, "An Iris biometric system for public and personal use," *IEEE Comput.*, vol. 33, no. 2, pp. 70–75, Feb. 2000.
- [9] J. W. Thompson, H. Santos-Villalobos, P. J. Flynn, and K. W. Bowyer, "Effects of Iris surface curvature on Iris recognition," in *Proc. 6th IEEE Int. Conf. Biometrics, Technol., Appl., Syst.*, 2013, pp. 1–3.
- [10] S. Baker, A. Hentz, K. Bowyer, and P. Flynn, "Degradation of Iris recognition performance due to non-cosmetic prescription contact lenses," *Comput. Vis. Image Understand.*, vol. 114, no. 9, pp. 1030–1044, 2010.
- [11] J. Daugman, "Demodulation by complex-valued wavelets for stochastic pattern recognition," *Int. J. Wavelets, Multiresolution Inf. Process.*, vol. 1, no. 1, pp. 1–17, 2003.
- [12] E. C. Lee, K. R. Park, and J. Kim, "Fake Iris detection by using purkinje image," in *Proc. IAPR Int. Conf. Biometrics*, 2006, pp. 397–403.
- [13] X. He, S. An, and P. Shi, "Statistical texture analysis-based approach for fake Iris detection using support vector machines," in *Proc. IAPR Int. Conf. Biometrics*, 2007, pp. 540–546.
- [14] Z. Wei, X. Qiu, Z. Sun, and T. Tan, "Counterfeit Iris detection based on texture analysis," in *Proc. 18th Int. Conf. Pattern Recognit.*, 2008, pp. 1–4.
- [15] Z. He, Z. Sun, T. Tan, and Z. Wei, "Efficient Iris spoof detection via boosted local binary patterns," in *Advances in Biometrics*. New York, NY, USA: Springer-Verlag, 2009, pp. 1080–1090.
- [16] H. Zhang, Z. Sun, and T. Tan, "Contact lens detection based on weighted LBP," in *Proc. 20th Int. Conf. Pattern Recognit.*, 2010, pp. 4279–4282.
- [17] J. Doyle, K. Bowyer, and P. Flynn, "Automated classification of contact lens type in Iris images," in *Proc. IEEE IAPR 6th Int. Conf. Biometrics*, Jun. 2013, pp. 1–6.
- [18] J. Doyle, K. Bowyer, and P. Flynn, "Variation in accuracy of textured contact lens detection," in *Proc. 6th IEEE Int. Conf. Biometrics, Technol., Appl., Syst.*, 2013, pp. 1–7.
- [19] CibaVision, Duluth, GA, USA. (2013, Apr.). *Freshlook Colorblends* [Online]. Available: <http://www.freshlookcontacts.com>
- [20] Bausch&Lomb, Rochester, NY, USA. (2014, Jan.). *Bausch&Lomb Lenses* [Online]. Available: <http://www.bausch.com>
- [21] LG, Riyadh, Saudi Arabia. (2011, Oct.). *Lg 4000 Camera* [Online]. Available: <http://www.lgiris.com>
- [22] IrisGuard, Washington, DC, USA. (2013, Apr.). *Ad100 Camera* [Online]. Available: <http://www.Irisguard.com/uploads/AD100ProductSheet.pdf>
- [23] Johnson&Johnson, Skillman, NJ, USA. (2013, Apr.). *Acuvue2 Colours* [Online]. Available: <http://www.acuvue.com/products-acuvue-2-colours>
- [24] C. Vision. (2013, Apr.). *Expressions Colors* [Online]. Available: <http://coopervision.com/contact-lenses/expressions-color-contacts>
- [25] VeriEye. (2005). *Iris Recognition Software* [Online]. Available: <http://www.neurotechnology.com/verieye.html>
- [26] T. Ojala, M. Pietikinen, and D. Harwood, "A comparative study of texture measures with classification based on feature distributions," *Pattern Recognit.*, vol. 29, no. 1, pp. 51–59, 1996.

- [27] M. Hall, E. Frank, G. Holmes, B. Pfahringer, P. Reutemann, and I. H. Witten, "The WEKA data mining software: An update," *SIGKDD Explorations Newsletter*, vol. 11, no. 1, pp. 10–18, 2009.
- [28] A. Bosch, A. Zisserman, and X. Munoz, "Representing shape with a spatial pyramid kernel," in *Proc. 6th ACM Int. Conf. Image Video Retr.*, 2007, pp. 401–408.



Daksha Yadav received the B.Tech. degree in computer science from the Indraprastha Institute of Information Technology Delhi, India, in 2013. She is currently pursuing the Ph.D. degree with the Lane Department of Computer Science and Electrical Engineering, West Virginia University, USA. Her research interests include image processing, machine learning, and biometrics.



Naman Kohli received the B.Tech. degree in computer science from the Indraprastha Institute of Information Technology Delhi, India, in 2013. He is currently pursuing the Ph.D. degree with the Lane Department of Computer Science and Electrical Engineering, West Virginia University, USA. His research interests include biometrics, computer vision, and pattern recognition.



James S. Doyle, Jr. received the B.Sc. degree in computer engineering from Purdue University, West Lafayette, IN, USA, and the M.Sc. degree in computer science and engineering from the University of Notre Dame, South Bend, IN, USA, in 2007 and 2011, respectively, where he is currently pursuing the Ph.D. degree with the Department of Computer Science and Engineering. His research interests include iris biometrics, pattern recognition, and computer vision.



She is also an Editorial Board Member of *Information Fusion*, Elsevier, and *EURASIP Journal on Image and Video Processing*, Springer. She is a member of the CDEFFS, Computer Society, and the Association for Computing Machinery. She is the recipient of 14 best paper and best poster awards in international conferences.



Mayank Vatsa received the M.S. and Ph.D. degrees in computer science from the West Virginia University, Morgantown, WV, USA, in 2005 and 2008, respectively. He is currently an Assistant Professor with the Indraprastha Institute of Information Technology Delhi, India. He has more than 100 publications in refereed journals, book chapters, and conferences. His research has been funded by the UIDAI and DIT. He is the recipient of the FAST Award from DST, India. His areas of interest are biometrics, image processing, computer vision, and information fusion. He is a member of the Computer Society and Association for Computing Machinery. He is the recipient of 14 best paper and best poster awards in international conferences. He is also an Associate Editor of *Information Fusion*, Elsevier, Area Editor of IEEE BIOMETRIC COMPENDIUM, and PC Cochair of the 2013 International Conference on Biometrics and the 2014 International Joint Conference on Biometrics.



Kevin W. Bowyer is the Schubmehl-Prein Professor of Computer Science and Engineering with the University of Notre Dame and also serves as the Chair of the Department. His research interests range broadly over computer vision and pattern recognition, including data mining, classifier ensembles, and biometrics. He received a 2014 Technical Achievement Award from the IEEE Computer Society, with the citation for pioneering contributions to the science and engineering of biometrics.

Over the last decade, he has made numerous advances in multiple areas of biometrics, including iris recognition, face recognition, and multibiometric methods. His research group has been active in support of a variety of government-sponsored biometrics research programs, including the Human ID Gait Challenge, the Face Recognition Grand Challenge, the Iris Challenge Evaluation, the 2006 Face Recognition Vendor Test, and the Multiple Biometric Grand Challenge. His most recent book is the *Handbook of Iris Recognition*, edited with Dr. Mark Burge.

Prof. Bowyer is a fellow of the IAPR and a Golden Core Member of the IEEE Computer Society. He is serving as the General Chair of the 2015 IEEE International Conference on Automatic Face and Gesture Recognition. He has previously served as the General Chair of the 2011 IEEE International Joint Conference on Biometrics, the Program Chair of the 2011 IEEE International Conference on Automatic Face and Gesture Recognition, and the General Chair of the IEEE International Conference on Biometrics Theory Applications and Systems from 2007 to 2009. He has also served as an Editor-in-Chief of the IEEE TRANSACTIONS ON PATTERN ANALYSIS AND MACHINE INTELLIGENCE and the IEEE BIOMETRICS COMPENDIUM, and is currently serving on the editorial board of IEEE ACCESS.